Effect of Film Thickness and Electrode Area on the Dielectric Breakdown Characteristics of Metallized Capacitor Films

Ilkka Rytöluoto & Kari Lahti
Tampere University of Technology (TUT)
Department of Electrical Engineering (DEE)
P.O. Box 692
FI-33101 Tampere, Finland

Abstract
An alternative approach for measuring breakdown characteristics of metallized and non-metallized polymer films has been previously developed at TUT. The method enables measurement of multiple breakdowns beyond the weakest point of each sample film by utilizing low-energy self-healing breakdown of metallized film. The method yields a large amount of breakdown data even from a relatively small sample area which enables the formation of detailed material-specific breakdown fingerprints. In this paper, some preliminary results of an ongoing further research on the area and thickness dependence of the breakdown characteristics of various polymer films are presented.

1. Introduction
Dielectric polymer films utilized in film capacitors are subjected to very high electric field stresses and thus, accurate statistical knowledge of their breakdown characteristics at the low breakdown probability region is of utmost importance in order to ensure safe and reliable design and operation in practice [1-4]. Breakdown measurement is typically realized as a short-term ramp-to-breakdown measurement and Weibull or other extreme-value distributions are then utilized for statistical analysis of the breakdown data [5]. However, weak spots in the polymer film due to the internal morphology and inherent properties of the polymer itself or due to extrinsic factors such as defects, voids, chemical impurities and non-ideal processing conditions can lead to a large deviation in the breakdown strength [6]. Moreover, the area and volume dispersion of the weak points in the film further complicates the dielectric strength evaluation [7-9]. Therefore, a large amount of breakdown data is required from a relatively large test area in order to gain a sufficient statistical relevance for practical applications. One approach for obtaining a large amount of breakdown data is to utilize an automatic breakdown strength measurement system such as in [10-11].
However, especially when the development and optimization phase of new dielectric materials such as polymer nanocomposites is considered, weak spots due to non-ideal processing conditions or other external factors may have a deteriorating effect on the dielectric breakdown strength [12]. Moreover, as the amount of sample material available for breakdown measurement may be scarce, the dielectric breakdown strength determined with only a small number of parallel samples may be misleading as it may be more representative of the weak spots due to extrinsic factors rather than a measure of the inherent properties of the material. Consequently, the true potential of the new dielectric may not be revealed completely.
In return to this problem, an alternative approach for measuring breakdown characteristics of thin polymer films has been previously developed at TUT [13]. The method is based on the concept of measuring multiple breakdowns per sample film beyond the weakest point (or dielectric strength) of each film by utilizing low-energy self-healing breakdown of metallized polymer film which effectively reduces the damage inflicted to the electrode layer with each consecutive breakdown. A data selection procedure based on the discharge energy behavior during self-healing of metallized dielectric film is utilized for validating mutual independence of the breakdown results prior to the statistical analysis. As a result, the method yields a large amount of breakdown data which enables the formation of detailed material-specific breakdown fingerprints.
The aim of this paper is to present the measurement method and some preliminary results of an ongoing further study on the area and thickness dependence of the breakdown characteristics of bi-axially oriented polypropylene (BOPP) and other capacitor-grade polymer films.

2. Background
Metallized film capacitors, which comprise of dielectric polymer films with thin metal electrodes evaporated directly on the film surface, have a unique ability to undergo self-healing breakdown [4]. During a breakdown in the dielectric film, a portion of the stored charge is discharged through the breakdown channel and consequently, a small area of the thin metallization layer around the fault spot is vaporized (Fig.1). As a result, the fault spot is spontaneously isolated from the rest of the electrode and insulation capability of the film is restored.

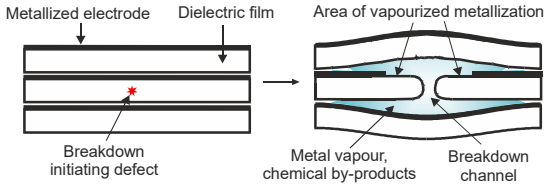

Fig.1. Self-healing breakdown in metallized polymer film.

Self-healing breakdown of metallized film has been extensively studied in the past literature and various factors have been found to affect the self-healing breakdown process [14-18]. The self-healing process may be characterized by the energy E_{SH} discharged during a self-healing event and it may be expressed as:

$$E_{SH} = \frac{kU^b C}{R_s^c \alpha(P)} = aU^b, \quad (1)$$

where U is the voltage, C is the capacitance, R_s is the metallization sheet resistance, $\alpha(P)$ is a function which relates inter-layer pressure to the discharge energy and a, b, c and k are experimentally definable constants.

2. Experimental

2.2. Test capacitor structure

A film arrangement comprising of two sheets of metallized film was used to form a test capacitor with an active area of A=2-42cm^2 (Fig. 2). The test film was placed at the bottom with the metallized side facing down. Another metallized film with the metallization facing down was then laid on the test film. A dielectric spacer film (polyimide, 100 µm in thickness) was used to separate the films at the region where the top film overlaps with the edge of the bottom film in order to prevent a flashover across the electrode edges. The film arrangement was then sandwiched between two sheets of thick transparent film in order to support the arrangement mechanically. The whole film arrangement was then laid on the bottom plate of the test capacitor unit and electrical contacts to the metallized films were made by means of aluminum clamp electrodes at the both ends of the bottom plate. Finally, a lightweight top plate made of transparent acrylic plastic was then laid on the top of the structure for further mechanical support (not shown in Fig. 2). Mechanical support was found to be very important when self-healing breakdown takes place in the test film, as the sudden pressure build-up during a self-healing breakdown event tends to shift and corrugate the films easily.

The measurement circuit used for the breakdown analysis is presented schematically in Fig. 3. In the test circuit, the test capacitor unit is depicted as the capacitance C_{DUT}. The purpose of the parallel capacitance C_P is to act as a fast charge storage buffer during a breakdown in the test capacitor. When a

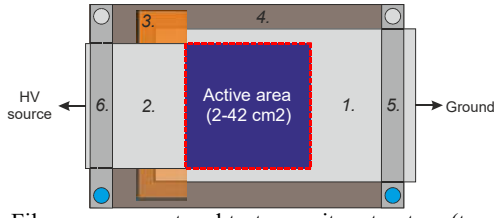

Fig.2. Film arrangement and test capacitor structure (top view). **1-2:** Metallized film (metallized surface facing down), **3:** Dielectric spacer film, **4:** Bottom plate, **5-6:** Aluminum clamp electrode (to high voltage source and ground).

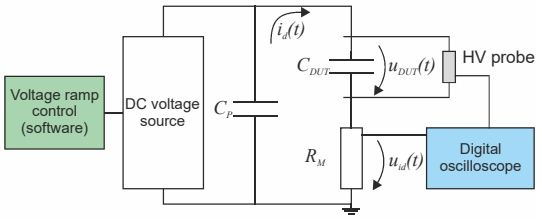

Fig.3. Measurement circuit for the breakdown measurement.

breakdown occurs in the test capacitor, a portion of the charge stored in the total capacitance $C=C_P+C_{DUT}$ is rapidly discharged at the fault spot. The discharge current $i_d(t)$ is then measured with an impulse current measurement resistor R_M as voltage signal $u_{id}(t)$. Simultaneously, the voltage $u_{DUT}(t)$ across the test capacitor is measured with a high voltage probe. Discharge current and test capacitor voltage during each self-healing event were recorded with an oscilloscope operating in sequence acquisition mode and triggered to the rising edge of the discharge current signal. The discharge energy E_{SH} could then be calculated by integrating the test capacitor voltage and the discharge current over the whole discharge duration τ:

$$E_{SH} = \int_0^\tau u_{DUT}(t) i_d(t) dt. \quad (2)$$

2.3. Measurement of multiple breakdowns

In order to enable convenient measurement of multiple self-healing breakdowns from the same sample area, a low level of discharge energy per each self-healing breakdown is desired, as it results in smaller de-metallized area around each breakdown site and reduced damage to the surrounding metallized layer. As also suggested by Eq. (1), there are various ways to affect the discharge energy during a self-healing breakdown. In this study, low-energy self-healing was realized by minimizing the total capacitance $C=C_P+C_{DUT}$ in the self-healing circuit. Thus, as the total charge available during the breakdown process is limited, a major voltage drop will occur across the test capacitor during each self-healing breakdown which effectively reduces the power density of the breakdown arc and leads to a rapid constriction of the breakdown arc. The effect of total capacitance on the discharge energy was studied in more detail in [13]. In this study, C_P=0-3.3nF was used in the measurement circuit in order to ensure that a sufficiently large discharge current pulse was measurable from the test capacitor terminals (clear trigger condition).

The progression of the breakdown measurement is illustrated schematically in Fig. 4. DC voltage is ramped from zero (Fig. 4a) with a constant speed of 30V/s until the voltage U_{DBS} corresponding to the dielectric breakdown strength of the film sample is reached and the first breakdown occurs in the film (Fig. 4b). As the voltage is increased beyond the first breakdown, more breakdowns begin to occur at an increasing frequency (Fig. 4c) until finally, the electrical contact is lost due to de-metallization at the active area and contact edges near the aluminum electrode clamps (Fig. 4d).

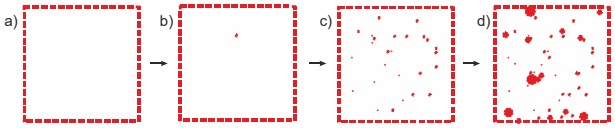

Fig.4. Progression of the breakdown measurement. The square area represents the active area of the test capacitor and the red spots depict the breakdown evolution as the voltage is increased. **a)** Beginning of test, U=0, **b)** first self-healing breakdown, U=U_{DBS}, **c)** multiple self-healings, U>U_{DBS}, **d)** end of test.

As multiple self-healing breakdowns are measured per sample area, only the breakdowns which appear independent should be chosen for further statistical analysis. One approach for the selection is to analyze the discharge energy behavior of the measured self-healing breakdowns on the basis of the power dependence $E_{SH}=aU^b$ [13]. The concept of the procedure is best described graphically, as shown in Fig. 7, in which the calculated discharge energies E_{SH} of all breakdowns measured from 25 samples of metallized BOPP (thickness d=6µm, C_P=0.5nF, $C_{DUT}=\varepsilon_0\varepsilon_r A/d$=3.25nF) are shown as a function of the breakdown voltage U_{BD}. Only those breakdowns are chosen (i) for which the corresponding discharge energies follow the trend preset by the first measured self-healing breakdowns and (ii) for which the breakdown voltage is higher than the dielectric strength of the sample. A physical explanation for the lower-than-expected discharge energies or breakdown voltages is that those breakdowns may have occurred near previous breakdown sites, resulting in lower discharge energy as the electrode layer around the breakdown site is already deteriorated or de-metallized. These breakdowns may also be attributed to successive self-healing taking place at the same breakdown site, presumably due to graphite formation and incomplete self-healing [17]. Non-breakdown events (partial discharges, surface flashovers etc.) may also be easily distinguished and disregarded with the discharge energy analysis.

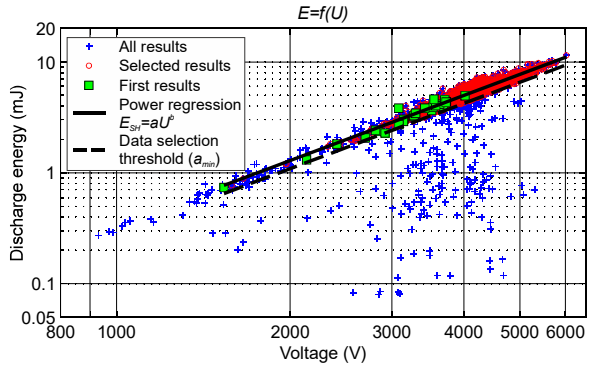

Fig. 7. Example of the data selection. The plot shows the calculated discharge energies of all the low-energy self-healing breakdowns measured from 25 samples of 6 µm metallized BOPP, A=10 cm^2 (blue). The first breakdowns (green) are used to determine the slope b of the power regression line (solid line, $E=aU^b$). By taking the energy variation of the first breakdowns into account, a_{min} is determined and used as a threshold (dashed line). Only the breakdowns with discharge energies above the threshold and with breakdown voltages higher than the first breakdown of the sample are chosen (red).

2.4. Statistical analysis

For the statistical analysis of the breakdown data in this study, 2-parameter Weibull distributions and additively mixed Weibull distributions were utilized. The cumulative distribution function of a 2-parameter Weibull distribution is of form [5]:

$$F(x)=1-\exp\left\{-\left(\frac{x}{\alpha}\right)^{\beta}\right\},\ x\geq 0, \qquad (3)$$

where x is the measured variable (e.g. breakdown voltage), α is the scale parameter which corresponds to the value of x at 63.2% failure probability and β is the shape parameter depicting the slope of the theoretical distribution. The cumulative distribution function of an additively mixed 2-parameter Weibull distribution is of form [5]:

$$F(x)=\sum_{i=1}^{S}\frac{N_i}{N}F_i(x), \qquad (4)$$

where $F_i(x)$ is the Weibull distribution from Eq. (3), S is the number of subpopulations, N_i/N is the portion (%) of the subpopulation i and α_i and β_i are the Weibull parameters of subpopulation i. A more detailed description of the distributions, parameter estimation and goodness-of-fit tests is out of the scope of this paper and can be found elsewhere.

2.5. Sample details

A collection of preliminary results of an ongoing study on the area and thickness dependence of the breakdown characteristics of various polymer films is presented in this paper. Various commercial-grade metallized polymer films have been studied, including BOPP, PEN (polyethylene naphthalate) and PPS (polyphenylene sulfide) films in the thickness range of 4 to 13.8µm. Metallized films were tested in dry conditions with the film arrangement presented in sub-chapter 2.2. In addition, the measurement technique was applied to a non-metallized 13.8µm hazy BOPP film by using metallized BOPP-12 films as electrodes above and under the test film with the metallized sides facing towards the non-metallized test film. These preliminary measurements were performed in mineral oil in order to mitigate surface flashovers above the ~5kV voltage range. Specifications of the studied films are given in Table 1. Film thickness and relative permittivity values were taken from the film data sheets.

Table 1. Specifications of the sample films.

Dielectric	Thickness (µm)	ε_r (1 kHz)	Metallization	Sheet resistance (Ω/□)
BOPP-12	12	2.2	Zn-Al alloy	5-12
BOPP-6	6	2.2	Zn-Al alloy	5-12
BOPP-4	4	2.2	Al	5
PEN	4	3.1	Al	5
PPS	4	3.0	Al	5
BOPP-13.8	13.8	2.2	-	-

3. Results and discussion

The area dependence of the breakdown results was studied in more detail with BOPP-6 and BOPP-12 films. The studied active areas included 2, 10, 24 and 42cm^2 for BOPP-6 and 2 and 24cm^2 for BOPP-12 (25 samples per active area). BOPP-6 and BOPP-12 films were obtained from the same manufacturer and they were of the same film type. Regarding to the other studied films, results measured with only one active area per film type are presented in this paper (A=16 or 20cm^2). When considering the thickness range of all the studied films as a whole, some implications on the thickness dependence of the results may also be given.

3.2. Area and thickness dependence

3.2.1 Dielectric strength

Firstly, Weibull plots of the dielectric strengths (first measured breakdowns) of the studied films are presented in Fig. 8 and the corresponding Weibull parameters are given in Table 2. Regarding to BOPP-6, the area dependence may be clearly seen in Fig. 8 at the higher probability region (>10%) which is also supported by the decreasing α and relatively constant β values with increasing area (Table 1). On the other hand, BOPP-12 clearly shows high β value for small active area but with larger area, β decreases considerably which implies that Weibull area scaling law does not apply (β should stay constant [5, 10]). It is also interesting to notice that BOPP-4 shows lower α and β values in comparison to the thicker BOPP films. PEN and PPS films show lower dielectric strengths in comparison to the BOPP films, however, PEN-4 shows exceptionally homogeneous breakdown distribution (high β). Lastly, especially the breakdown data points of BOPP-6 and BOPP-12 show deviation from the single Weibull distributions at the low-probability region (see Fig. 8). Similar deviation from a single Weibull distribution has been previously reported for e.g. BOPP, PI (polyimide) and PTFE (polytetrafluoroethylene) films [11, 19-20]. This deviation suggests that the breakdowns may be due to more than one breakdown mechanisms and that a single 2-parameter Weibull distribution is in fact insufficient for representing such a breakdown data set.

3.2.2 Characteristic breakdown distributions

The characteristic breakdown probability distributions

Table 2. Weibull-parameters of the dielectric strengths of the studied films (first measured breakdowns).

BOPP-6					
Area (cm^2)	2*	10*	16**	24*	42*
α (V/µm)	679	567	596	547	505
β	12.15	7.74	11.16	10.40	7.80
BOPP-12					
Area (cm^2)	2*	24*			
α (V/µm)	709	607			
β	18.85	6.17			
	BOPP-4** (16cm^2)	**PEN-4**** (16cm^2)	**PPS-4**** (16cm^2)	**BOPP-13.8**** (20cm^2)	
α (V/µm)	555	365	341	613	
β	6.31	36.15	10.89	10.48	

*) 25 samples/area
**) 10 samples/area

obtained with the low-energy self-healing breakdown measurement method are shown in Fig. 9a and Fig. 9b for BOPP-6 and BOPP-12, respectively, and in Fig. 9c for the other films. Breakdown fields corresponding to 50% breakdown probabilities of the mixed distributions are shown in Fig. 10 as a function of electrode area for comparison. The number of breakdowns considered from each measured film sample was limited to 50 (if less breakdowns were obtained, all of them were taken into consideration). The data selection procedure was then applied to the selected breakdowns (see sub-chapter 2.3) and mixed Weibull distributions were fitted to the selected breakdowns on the basis of the best goodness-of-fit test result. Detailed description of the discharge energies, data selection procedure, Weibull parameter estimation, distribution fitting and the structure of the mixed distributions is out of the scope of this paper and will be covered in a future publication. In regard to BOPP-6, the aforementioned issues and the evolution of the structure of the mixed Weibull distribution with increasing active area have been previously analyzed in [13].

As the measurement method yields a large amount of breakdown data from a relatively small amount of samples, the empirical breakdown distributions shown in Fig. 9 are very detailed and various different types of breakdown patterns may be identified, similarly as in [7], [8], [11] and [20]. For example, BOPP-6 clearly shows a distinct defect population at the low-probability region which can be seen as the curvature (or S-shape) of the theoretical distributions (Fig. 9a). As the electrode area (or total measured area) is increased, the amount of low-field low-probability breakdowns increases whereas the

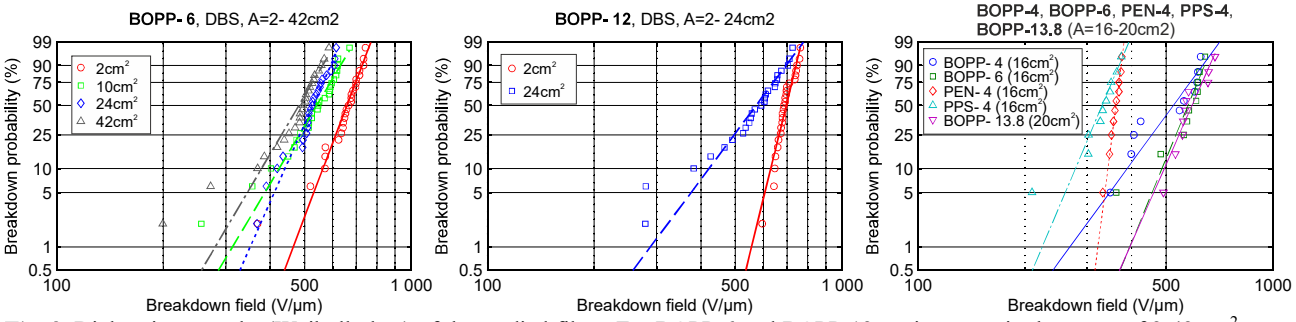

Fig. 8. Dielectric strengths (Weibull plots) of the studied films. For BOPP-6 and BOPP-12, active areas in the range of 2-42 cm^2 were used (25 measurements per area). For the other films, measurements were made with 16 or 20 cm^2 (10 measurements per area).

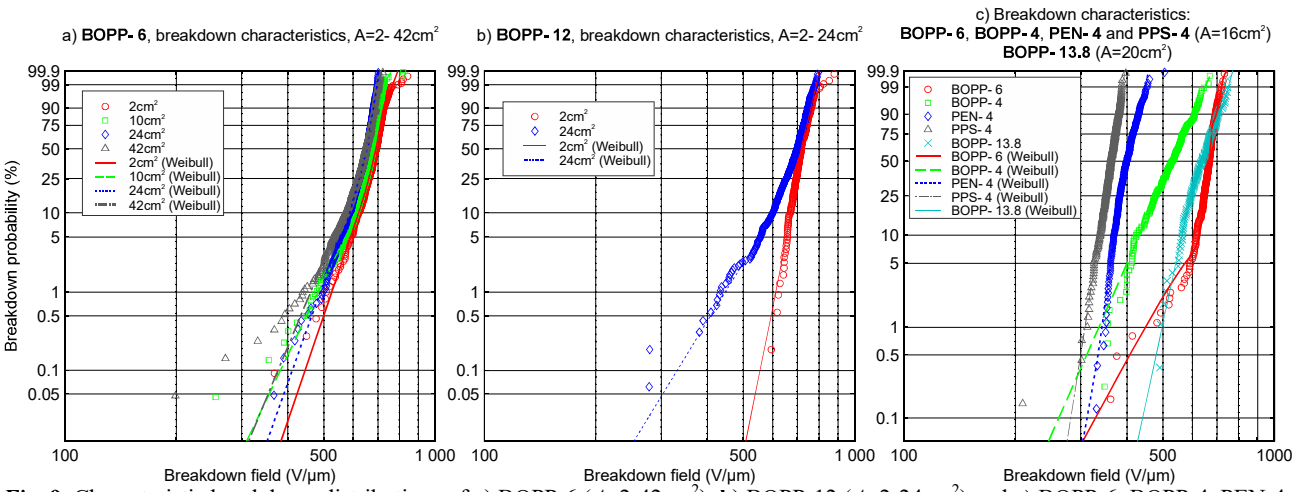

Fig. 9. Characteristic breakdown distributions of **a)** BOPP-6 (A=2-42cm^2), **b)** BOPP-12 (A=2-24cm^2) and **c)** BOPP-6, BOPP-4, PEN-4, PPS-4 and BOPP-13.8 (A=16-20cm^2). Multiple breakdowns were measured per each sample by utilizing low-energy self-healing breakdown. The number of breakdowns considered per each film sample was limited to 50. Mixed Weibull distributions were fitted to the breakdown data on the basis of the best goodness-of-fit test. The numbers of selected breakdowns were; **BOPP-6**: 546, 1103, 1040 and 1057 for 2, 10, 24 and 42cm^2 areas, respectively; **BOPP-12**: 271 and 811 for 2 and 24cm^2 areas, respectively; **BOPP-6**, **BOPP-4**, **PEN-4**, **PPS-4** (16cm^2) and **BOPP-13.8** (20cm^2): 225, 311, 396, 347 and 139, respectively.

high-probability parts (>10%) of the distributions, which may be attributed to the intrinsic breakdown strength of the polymer itself, exhibit only a slight shift towards lower dielectric strength but show no major change in distribution homogeneity. On the other hand, the results obtained from BOPP-12 samples clearly show that the breakdown distribution becomes more disperse with increasing area (Fig. 9b), as also suggested by the dielectric strength results (see Table 2 and Fig. 8.). In comparison to BOPP-6, the other studied materials do not show as clear defect populations and especially PEN and PPS films show very homogeneous distributions.

The breakdown results of the BOPP films (in the 4-13.8µm thickness range) also show that the breakdown distributions become more homogeneous with increasing thickness (Figs. 8-9). The effect is more profound with small areas (see 2cm^2 distributions for BOPP-6 and BOPP-12) and similar results have been previously reported for e.g. PI and BOPP films, for which the Weibull β increased with thickness [8, 19].

The breakdown distributions of the BOPP films also show a shift towards higher dielectric strength with increasing thickness. However, this is in contradiction to the inverse power law typically reported for solid dielectrics which proposes a decrease in dielectric strength with an increase in sample thickness [21].

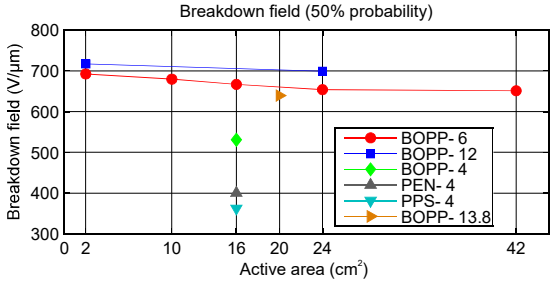

Fig. 10. Breakdown fields corresponding to the 50% breakdown probability for the studied materials as a function of electrode area. The values are based on the characteristic breakdown distributions presented in Fig. 9.

Recently, the statistical behavior of dielectric breakdown of polymers has been modeled based on the field-assisted percolation model which represents the amorphous, crystalline and free volume of polymer as a three-dimensional cubic lattice of randomly distributed traps with trap barriers in a certain range [22]. In the presence of an electric field the trap barriers are reduced which facilitates electron transfer and if the field is high enough, a percolation cluster leading to a dielectric breakdown can form across the material volume. The study showed that a small concentration of randomly distributed defects in the material volume can cause deviation from a single Weibull distribution and the defect population is more significant in large-area samples. This is coherent with the breakdown results obtained from BOPP-6 samples (Fig. 9a and Fig. 9c).

The field-assisted percolation model study also suggested the decrease of Weibull α and β values with decreasing simulated network size (sample volume) which is generally in a good agreement with the thickness dependence results obtained in this study. However, the fact that BOPP-12 first showed more homogeneous breakdown distribution in comparison to BOPP-6 with small active area, but that the effect was then mitigated when a larger sample area was measured, may be attributed to a defect population present in the BOPP-12 film. A more detailed analysis will be covered in a future publication.

4. Conclusion

A new dielectric breakdown measurement method for determining breakdown characteristics of polymer films was presented. The method is based on the measurement of multiple breakdowns per sample area beyond the weakest point of the film by utilizing low-

energy self-healing breakdown of metallized polymer film which effectively reduces the electrode loss during self-healing. The method yields a large amount of breakdown data which enables the formation of detailed material-specific breakdown fingerprints.

Breakdown characteristics of various metallized and non-metallized BOPP, PEN and PPS films in the thickness range of 4 to 13.8 µm were measured and analyzed with active areas in the range of 2 to 42 cm^2. Measurement of multiple breakdowns beyond the weakest point of each sample film enabled detailed dielectric breakdown characterization and comparison regardless of the weak points present in the films. Various types of breakdown patterns were observed and in most cases, single 2-parameter Weibull distributions were found to be insufficient for representing the breakdown data sets. Regarding to the studied BOPP films, the statistical analysis showed that defects in the films have a profound effect on the breakdown characteristics with increasing active area. Moreover, increase in film thickness was found to generally increase the breakdown strength and breakdown distribution homogeneity of BOPP films, especially with small active areas. The results obtained in this study underline the complex nature of the area and thickness dependence of dielectric breakdown characteristics of polymer films.

References

[1] M. Rabuffi and G. Picci, "Status quo and future prospects for metallized polypropylene energy storage capacitors," *Plasma Science, IEEE Transactions on*, vol. 30, no. 5, pp. 1939-1942, 2002.

[2] C.W. Reed and S.W. Cichanowski, "The fundamentals of aging in HV polymer-film capacitors," *Dielectrics and Electrical Insulation, IEEE Transactions on*, vol. 1, no. 5, pp. 904-922, 1994.

[3] W.J. Sarjeant, J. Zirnheld, and F.W. MacDougall, "Capacitors,", vol. 26, no. 5, pp. pp.1368-1392, 1998.

[4] S.A. Boggs, J. Ho, and T.R. Jow, "Overview of laminar dielectric capacitors," *Electrical Insulation Magazine, IEEE,* vol. 26, no. 2, pp. 7-13, 2010.

[5] Hauschild W. and Mosch W., *Statistical Techniques for High-Voltage Engineering*. Philadephia: Institution of Engineering and Technology, 1992.

[6] L. A. Dissado and J. C. Fothergill, *Electrical Degradation and Breakdown in Polymers*. Philadelphia: Peter Peregrinus Ltd., 1992.

[7] S.J. Laihonen, U. Gafvert, T. Schutte, and U.W. Gedde, "Influence of electrode area on dielectric breakdown strength of thin poly(ethylene terephthalate) films," in *Electrical Insulation and Dielectric Phenomena, 2004. CEIDP '04. 2004 Annual Report Conference on*, 2004, pp. 563- 567.

[8] S.J. Laihonen, U. Gafvert, T. Schutte, and U.W. Gedde, "DC breakdown strength of polypropylene films: Area dependence and statistical behavior," *Dielectrics and Electrical Insulation, IEEE Transactions on*, vol. 14, no. 2, pp. 275-286, 2007.

[9] S. Ul-Haq and G.R.G. Raju, "Weibull statistical analysis of area effect on the breakdown strength in polymer films," in *Electrical Insulation and Dielectric Phenomena, 2002 Annual Report Conference on*, 2002, pp. 518-521.

[10] Chunchuan Xu, Janet Ho, and S. Boggs, "Automatic breakdown voltage measurement of polymer films," *Electrical Insulation Magazine, IEEE*, vol. 24, no. 6, pp. 30-34, 2008.

[11] S.J. Laihonen, A. Gustafsson, U. Gafvert, T. Schutte, and U.W. Gedde, "Area dependence of breakdown strength of polymer films: automatic measurement method," *Dielectrics and Electrical Insulation, IEEE Transactions on*, vol. 14, no. 2, pp. 263-274, 2007.

[12] C. Calebrese, Le Hui, L.S. Schadler, and J.K. Nelson, "A review on the importance of nanocomposite processing to enhance electrical insulation," *Dielectrics and Electrical Insulation, IEEE Transactions on*, vol. 18, no. 4, pp. 938-945, 2011.

[13] I. Rytöluoto and K. Lahti, "New Approach to Evaluate Area-Dependent Breakdown Characteristics of Dielectric Polymer Films," *Dielectrics and Electrical Insulation, IEEE Transactions on*, 2013, in press.

[14] H. Heywang, "Physikalische und chemische Vorgänge in selbstheilenden Kunststoff-Kondensatoren," *Colloid & Polymer Science*, vol. 254, no. 2, pp. 139-147, 1976.

[15] J.H Tortai, A. Denat, and N. Bonifaci, "Self-healing of capacitors with metallized film technology: Experimental observations and theoretical model," *Journal of Electrostatics*, vol. 53, no. 2, pp. 159-169, 2001.

[16] P.-O. Sassoulas, B. Gosse, and J.-P. Gosse, "Self-healing breakdown of metallized polypropylene," in *Solid Dielectrics, 2001. ICSD '01. Proceedings of the 2001 IEEE 7th International Conference on* , 2001, pp. 275-278.

[17] B. Walgenwitz, J.-H. Tortai, N. Bonifaci, and A. Denat, "Self-healing of metallized polymer films of different nature," in *Solid Dielectrics, 2004. ICSD 2004. Proceedings of the 2004 IEEE International Conference on*, 2004, pp. 29-32.

[18] J.-H. Tortai, N. Bonifaci, A. Denat, and C. Trassy, "Diagnostic of the self-healing of metallized polypropylene film by modeling of the broadening emission lines of aluminum emitted by plasma discharge," *Journal of Applied Physics*, vol. 97, no. 5, 2005.

[19] S. Diaham et al., "Dielectric breakdown of polyimide films: Area, thickness and temperature dependence," *Dielectrics and Electrical Insulation, IEEE Transactions on*, vol. 17, no. 1, pp. 18-27, 2010.

[20] G. Raju, A. Katebian, and S.Z. Jafri, "Breakdown voltages of polymers in the temperature range 23°-250°C," *Dielectrics and Electrical Insulation, IEEE Transactions on*, vol. 10, no. 1, pp. 117-127, 2003.

[21] G. Chen, Z. Junwei, S. Li, and L. Zhong, "Origin of thickness dependent dc electrical breakdown in dielectrics," *Applied Physics Letters*, vol. 100, no. 22, 2012.

[22] K. Wu, Y. Wang, Y. Cheng, L.A. Dissado, and X. Liu, "Statistical behavior of electrical breakdown in insulating polymers," *Journal of Applied Physics*, vol. 107, no. 6, 2010.

[23] D.G. Shaw, S.W. Cichanowski, and A. Yializis, "A Changing Capacitor Technology - Failure Mechanisms and Design Innovations," *Electrical Insulation, IEEE Transactions on*, vol. EI-16, no. 5, pp. 399-413, 1981.